Relaxation dynamics induced in glasses by absorption of hard x-ray photons

G. Pintori,[1,*] G. Baldi,[1] B. Ruta,[2,3] and G. Monaco[1]
[1]*Dipartimento di Fisica, Trento University, Povo, Trento I-38123, Italy*
[2]*ESRF—The European Synchrotron, CS 40220, 38043 Grenoble Cedex 9, France*
[3]*Univ. Lyon, Université Claude Bernard Lyon 1, CNRS, Institut Lumière Matière, F-69622 Villeurbanne, France*

(Received 5 April 2017; revised manuscript received 19 February 2019; published 26 June 2019)

X-ray photon correlation is used to probe the slow dynamics of the glass-former B_2O_3 across the glass transition. In the undercooled liquid phase, the decay times of the measured correlation functions are consistent with visible light-scattering results and independent of the incoming flux; in the glass they are instead temperature independent and show a definite dependence on the x-ray flux since here the dynamics is artificially induced by the interaction with the x-ray beam. The decay times in this regime provide a measure of the number of atoms that rearrange on a length scale on the order of the inverse of the exchanged wave vector following an absorption event. Quite surprisingly, this number for the B_2O_3 glass is on the order of thousands of atoms. The induced dynamics persists also at higher temperatures until, close to the glass transition, it gets much slower than the intrinsic relaxation of the material. We suggest a possible scenario in which the single absorbed photon induces a collective motion of a volume of the glass with a size of the order of the nanometer.

DOI: 10.1103/PhysRevB.99.224206

I. INTRODUCTION

X-ray photon correlation spectroscopy (XPCS) is a powerful method for studying dynamics in disordered systems, giving access to length and timescales inaccessible by other techniques. The typical timescales are much longer than those probed by inelastic x-ray scattering, and the length scales are much shorter than those investigated by visible-light techniques [1]. XPCS requires the capability of third generation synchrotron radiation sources of producing coherent x-ray beams several orders of magnitude more intense than previously available [1]. The pioneering papers by Sutton *et al.* [2] and Brauer *et al.* [3] laid the foundations of this research area. XPCS has been used to study dynamics occurring on length scales >10 nm, for example, in small-angle scattering experiments on colloids and polymers or near Bragg peaks of crystals [4]. The capability to resolve single atomic motion in condensed matter with this technique has also been shown [5,6].

Much of the excitement about scattering with coherent x rays, however, arises from the perspective to perform atomic resolution correlation experiments to study the complex dynamics of disordered systems, whose archetypes are glasses. Their microscopic structures remain the object of active research. Among the works that laid the groundwork in this field are those of Zachariasen [7] and Warren [8]. The existence of short-range order in glasses was rather clear, whereas only the application of many different methods, such as neutron scattering, extended fine-structure x-ray absorption and Raman spectroscopy [9] has made it possible to provide hints into the medium-range order. For what concerns the dynamics, the glassy state is described as arrested with relaxation times too long to be observed on human timescales [10]. But what happens on the atomic scale? The works by Ruta *et al.* report the rather unexpected result that glasses display atomic rearrangements within a few minutes in both metallic [11] and silicate glasses [12] and this even in the deep glassy state.

Although the measured dynamics of metallic glasses seems a genuine structural relaxation of the material [11,13], in the oxide glasses at room temperature, the dynamics is simultaneously pumped and probed by the incident x-ray beam [14]. Specifically, the x-ray beam has sufficient intensity to induce an artificial atomic movement, most probably through the process of radiolysis. Here, we utilize XPCS to shed light on the effect of hard x rays on the dynamics at the atomic level in the network glass B_2O_3 across the glass transition. We show that this beam-induced dynamics competes with the structural relaxation, is negligible in the undercooled liquid phase, and dominant in the glass. The artificial dynamics induced by the beam can be described as a sequence of structural rearrangements involving the collective motion of up to thousands of atoms.

The paper is organized as follows. In Sec. II, we provide some details on the sample preparation and on the XPCS technique. Section III is devoted to the data analysis and to the discussion of the results. The conclusions are drawn in Sec. IV.

II. EXPERIMENT AND DATA ANALYSIS

The B_2O_3 glass used in this paper was prepared starting from 99%-purity B_2O_3 powder (Sigma-Aldrich), which was heated at 423 K and there kept for 16 h to reduce the water content. Water has, in fact, a large effect on the properties of the B_2O_3 glass [15,16]. The dehydrated powder was melted in air in an alumina crucible, and a clear bubble free melt was obtained after 4 h at 1230 K. It was quickly cooled to

*Corresponding author: giovanna.pintori@unitn.it

room temperature to produce a glass with a cooling rate on the order of 10 K/s. On cooling down, the melt was pressed between two metallic plates and subsequently mechanically polished to a thickness of $L = 180 \pm 20$ μm. The thickness was chosen to optimize the scattered intensity at 8.1 keV whereas keeping a reasonably good contrast in the wide angle geometry. A resistively heated furnace in vacuum was used to raise up the sample temperature with a final temperature stability of ± 0.05 K. The temperature was measured by a thermocouple close to the sample and monitored during the whole experiment.

XPCS measurements on the B_2O_3 glass former were performed at beamline ID10 at the European Synchrotron Radiation Facility (ESRF) in Grenoble (F). The 8.1-keV x-ray beam, produced by an undulator source, was monochromatized using a Si(111) channel cut (energy bandwidth $\Delta E/E \approx 1.4 \times 10^{-4}$) and then focused by a Be compound refractive lens at the sample position. Hard x rays originating from higher-order monochromator reflections were suppressed by a white beam double-mirror placed before the main monochromator. The spatially coherent part of the beam was selected by rollerblade slits opened to 10(H) × 8(V) μm^2, placed ~0.18 m upstream of the sample. This configuration leads to a beam with a longitudinal coherence length of ~1.1 μm and a transverse coherence length of ~4 (H) × 10(V) μm^2. The speckle patterns were collected in transmission geometry by two IkonM charge-coupled devices (CCDs) from Andor Technology (1024 × 1024 pixels, 13 × 13-μm^2 pixel size) installed perpendicularly to the horizontal scattering plane, ~67 cm downstream of the sample, and symmetrically arranged with respect to the incoming beam. The CCDs were both centered at a scattering angle corresponding to the maximum of the structure factor $Q_{\max} = 1.5$ Å^{-1}. All pixels of the CCDs were associated with the same wave-vector $Q_{\max}$ with an overall resolution of $\Delta Q = 0.04$ Å^{-1}.

The measurements were conducted by varying the flux of the incident beam F on the sample by means of different attenuators. Each attenuator made out of Si leads to a decrease in the beam flux by a factor of $\sim 1/e$. In particular, the atomic dynamics of the B_2O_3 glass was measured for: (i) no attenuator, corresponding to an incoming beam flux $F_0 = 8.6 \times 10^{10}$ ph/s per 200-mA current in the storage ring; (ii) a single attenuator filter, corresponding to a flux $F_1 = 2.6 \times 10^{10}$ ph/s per 200 mA; (iii) and a double-attenuator filter corresponding to a flux $F_2 = 9.8 \times 10^9$ ph/s per 200 mA. The intensity scattered by the B_2O_3 glass was collected for different temperatures in the 297–593-K range. At each temperature series, up to 3000 frames were taken with exposure times per frame Δt_e in the range of 2–7 s depending on the attenuator employed during the measurement. The recorded frames were subsequently analyzed by the multispeckle XPCS method [17,18] to obtain a set of temporal correlation functions. A series of normalized intensity autocorrelation functions $g_2(Q,t)$, measured in vitreous B_2O_3 by cooling the sample from the supercooled liquid phase to the glassy state ($T_g = 526$ K) using the full beam-flux F_0 is shown in Fig. 1. The dynamics becomes slower as the temperature is lowered down to 498 K and shows very little temperature dependence at lower temperatures. Moreover, the atomic motion in the glassy

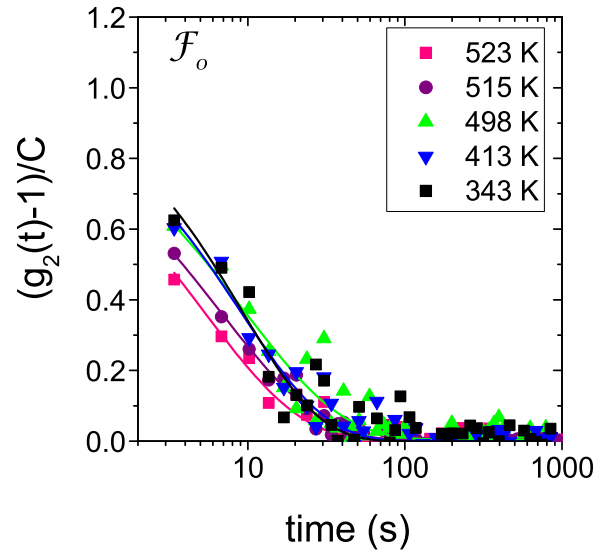

FIG. 1. Normalized intensity autocorrelation functions (symbols) measured at $Q_{\max} = 1.5$ Å^{-1} in B_2O_3 for different temperatures across $T_g = 526$ K together with the best-fitting stretched exponential line shapes. These measurements have been carried out with full beam flux F_0.

state at $T = 413$ K strongly depends on the x-ray beam flux as shown in Fig. 2, leading to an induced relaxation time that is shorter the higher the incident beam flux, similar to that reported in Ref. [14]. The induced dynamics is independent of the global dose released on the sample, at least, up to the maximum doses of $\simeq 2$ GGy reached during the measurements. This beam-induced effect is also not related to any visible structural damage as shown in Fig. 3. Here, the $I(Q)$ data measured on the same spot at the beginning and at the end of a XPCS scan are compared. The scan duration corresponds to an accumulated dose of 2.2 GGy, and the scattered intensity

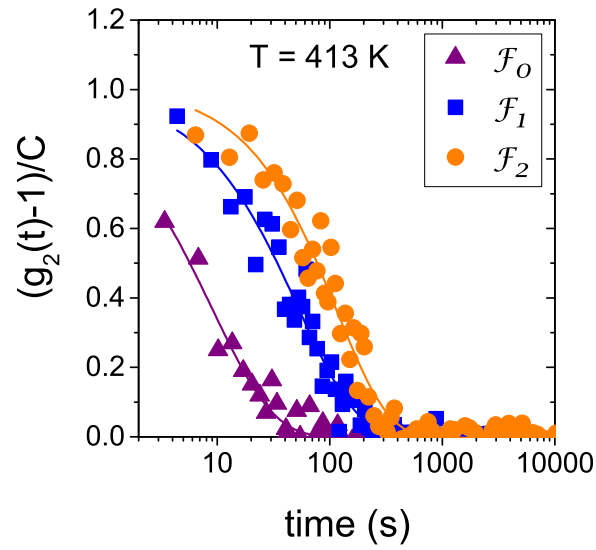

FIG. 2. Normalized intensity autocorrelation functions (symbols) measured at $T = 413$ K and $Q_{\max} = 1.5$ Å^{-1} for different incoming beam fluxes, see the legend together with the best-fitting stretched exponential line shapes.

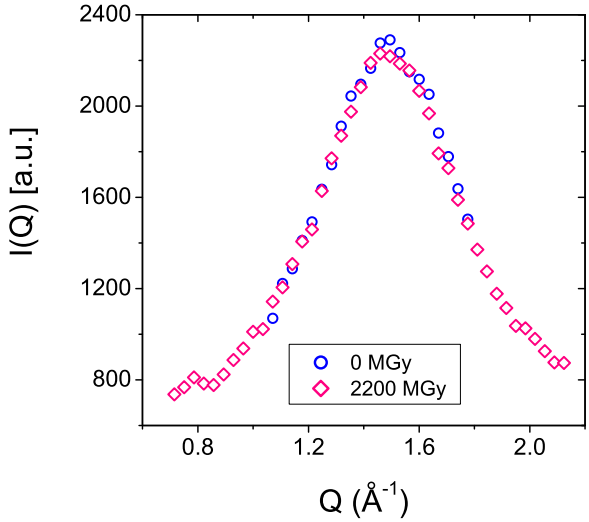

FIG. 3. Total scattered intensity profile measured in B_2O_3 on a fresh spot (circles) and after a dose of ∼2.2 GGy (lozenges). The data are normalized by the incoming beam intensity after background subtraction.

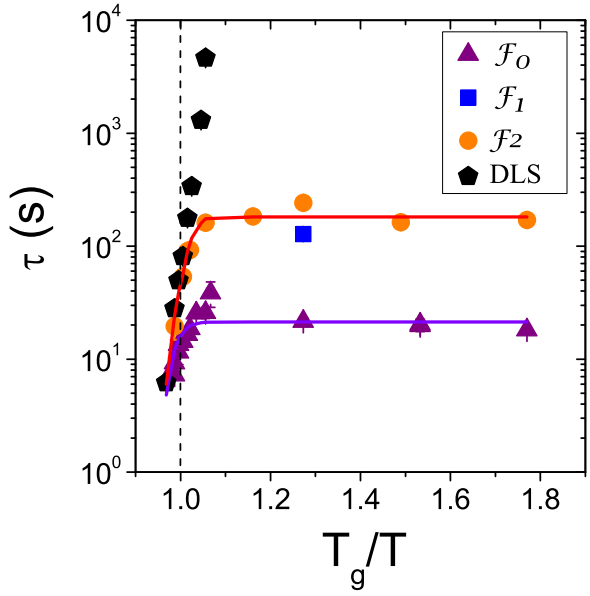

FIG. 4. Decay time measured using XPCS in B_2O_3 at $Q_{max} = 1.5$ Å^{-1}. Different symbols for the XPCS data refer to different x-ray beam fluxes as reported in the legend. The black pentagons are macroscopic data obtained using dynamic light scattering [22]. The solid lines are obtained using Eq. (2) and refer to the XPCS data measured with the lowest and highest beam fluxes. The dashed vertical line marks the position of T_g.

is stable within 2% accuracy. Moreover, the timescale of the beam-induced dynamics reversibly changes with the incident flux as also shown in Ref. [14] for the case of SiO_2.

III. RESULTS AND DISCUSSION

The shape of the correlation functions can be quantified by fitting to the data the Kohlrausch-Williams-Watts (KWW) expression [19,20],

$$g_2(Q,t) = 1 + \mathcal{C}(Q)\exp[-2(t/\tau)^{\beta}], \tag{1}$$

where $\mathcal{C} = \mathcal{B}(Q)f_Q^2$ is the product of the experimental contrast and the square of the nonergodicity factor, β is the shape parameter, and τ is the characteristic decay time. Only a few curves show the full decay from $1+\mathcal{C}$ to 1: Most of them show, in fact, only the tail of the curve with a decay time that is fast on the scale fixed by the exposure time per frame Δt_e. The fitting analysis of the experimental curves using Eq. (1) has then been carried out using all free fitting parameters ($\mathcal{C}$, τ, and β) only for the curves with longer τ. For these curves, the parameter $\mathcal{C}$ comes out to be only little scattered around a mean value of $\mathcal{C} = (8.5 \pm 0.4) \times 10^{-3}$. This value is lower than that observed in other glasses [11,12] because we had to use thicker samples in order to maximize the scattered intensity. Recalling that the nonergodicity factor f_Q in correspondence to the maximum of the structure factor is expected to display only a weak temperature dependence (e.g., see Ref. [21]), the fits to all experimental curves have been carried out using the previously mentioned fixed value for $\mathcal{C}$. The temperature dependence of the decay time is reported in Fig. 4. Macroscopic values (black pentagons) have been obtained from measurements carried out with dynamic light scattering (DLS) [22]. Different symbols for the XPCS data refer to different beam intensities as reported in the legend. We highlight three main observations: (i) Above T_g, the XPCS relaxation time τ_X is very close to that measured in the visible range and with very similar temperature dependence confirming previous measurements on other systems [11,12,23]. (ii) In the glassy state, τ_X is almost temperature independent and remains in the 10–100-s range. These findings are very similar to the behavior recently observed in other network glasses [12,14,24] on the atomic length scale, contrary to the expectation of an almost arrested dynamics. (iii) Whereas in the supercooled liquid region, all of the XPCS data basically overlap, and in the glassy state we observe different values of τ_X depending on the incident beam flux. However, there is no clear evidence of radiation damage (meaning permanent damage): The beam flux simply fixes the timescale of the dynamics [14].

In order to discriminate the beam-induced dynamics from the equilibrium dynamics, we can use a simple model where the decorrelation time measured with XPCS is written as

$$\frac{1}{\tau_X} = \frac{1}{\tau} + \frac{1}{\tau_{\rm ind}}, \tag{2}$$

where τ is the structural relaxation time of B_2O_3 and $\tau_{\rm ind}$ is the beam-induced decorrelation time. We can use, for $\tau_{\rm ind}$, a temperature-independent (but beam-flux-dependent) value given by τ_X in the glass; and for τ, the values obtained by photon correlation in the visible range and extrapolated below T_g. Figure 4 shows that this simple model (solid lines) describes very well the measured τ_X data. The beam-induced dynamics takes place in parallel to the spontaneous sample dynamics: Above the glass transition temperature, the structural relaxation is the fastest process and, therefore, dominates, whereas below T_g, it becomes completely irrelevant. The shape parameter β, extracted from the KWW fits, is shown in Fig. 5. For the incoming beam-flux F_2, the obtained values

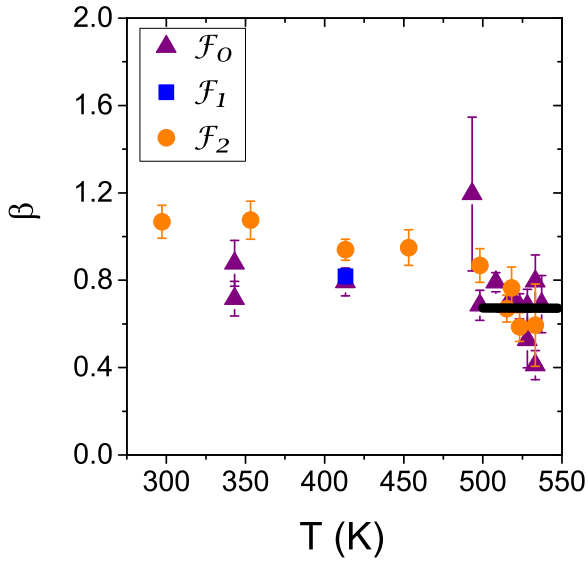

FIG. 5. Temperature dependence of the shape parameter β for B_2O_3 at $Q_{max} = 1.5$ Å^{-1}. The different symbols refer to different beam fluxes, see the legend. The full line indicates the mean value obtained with visible light scattering in the range of 500–550 K [22].

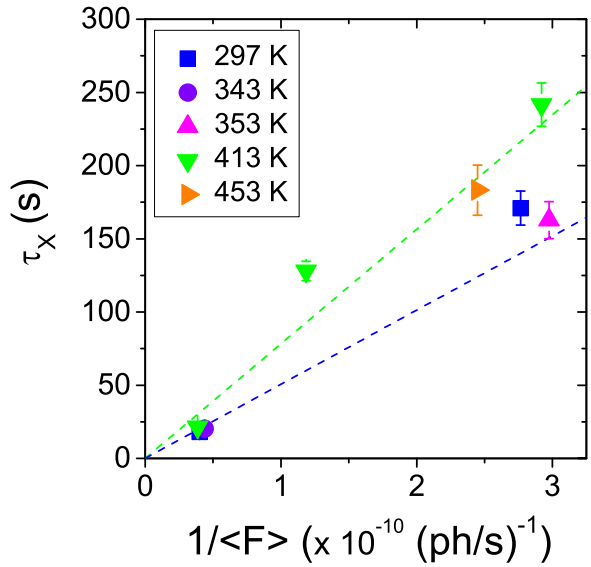

FIG. 6. Decay time obtained from the XPCS measurements in B_2O_3 at $Q_{max} = 1.5$ Å^{-1} as a function of the inverse of the average flux. Different symbols refer to different temperatures, see the legend. The best-fitting lines for $T = 413$ and $T = 297$ K are also reported.

for β are basically temperature independent in the glass with a mean value of $\beta = 0.97 \pm 0.04$. At higher temperatures, they decrease to reach a value which is compatible with the average equilibrium value of 0.67 ± 0.09 obtained with visible light scattering [22] on a B_2O_3 sample prepared by exactly the same method as reported here. The reduction of β in the XPCS data is, therefore, here another sign of the transition from a beam-induced dynamics in the glass to the equilibrium dynamics in the undercooled liquid. The β values at higher fluxes are affected by a considerable uncertainty because the decorrelation is faster and only a portion of the curve is measured. Taking this into account, we conclude that the β parameter does not show an appreciable dependence on the flux in the entire explored temperature range. It is, however, interesting to observe that, different from the case of silica and germania [14], the shape parameter for the beam-induced decay corresponds to a simple exponential rather than a compressed ($\beta > 1$) one.

In the glassy state, the decay time obtained by XPCS is only a little temperature dependent and clearly decreases on increasing the x-ray beam flux as shown in Fig. 4. In particular, our data are compatible with the expression $\tau_X \propto \langle F \rangle^{-1}$, see the points corresponding to 413 K in Fig. 6. Here, $\langle F \rangle = F\, \Delta t_e/\Delta t_l$ is the average x-ray flux arriving at the sample; and Δt_l is the lag time, i.e., the sum of the exposure time Δt_e and the readout time $\Delta t_r = 1.4$ s. Figure 6 confirms the results already reported in Ref. [14] for the case of the silica and germania glasses.

We can also rephrase the previous observation by stating that the relaxation time measured by XPCS is inversely proportional to the average number of photons absorbed by the B_2O_3 sample, i.e., $\tau \propto \langle F \rangle_a^{-1}$, where $\langle F \rangle_a = \langle F \rangle [1 - \exp(-\mu L)]$, μ is the attenuation coefficient for B_2O_3 at 8.1 keV, and L is the sample thickness. It is then easy to clarify the meaning of this relation. In fact, from the definition of intensity autocorrelation function, we know that in a time τ_X, N_{tot}/e of B_2O_3 units move by a distance $1/Q$, where N_{tot} is the number of units in the scattering volume. More precisely, in a time τ_X, $f_Q N_{tot}/e$ of units move by a distance $1/Q$. However, f_Q is very close to 1 when Q is close to the maximum of the structure factor (e.g., see Ref. [21]), and, therefore, we can neglect its presence in what follows. We also know that the number of photons absorbed in time τ_X is obviously $\langle F \rangle_a \tau_X$. Consequently, the number of units N_u that move after the absorption of one photon is the ratio of the number of units that move by a distance $1/Q$ in time τ_X and the number of photons absorbed in the same time,

$$N_u = \frac{1}{e} \frac{N_{tot}}{\langle F \rangle_a \tau_X}. \tag{3}$$

The number N_{tot} can be calculated using the sample mass density $\rho = 1.83$ g/cm^3 and the scattering volume defined by the beam spot size and the sample thickness. The values for N_u obtained in this way are reported in Fig. 7 as a function of temperature in the range where the observed dynamics is beam induced, i.e., for $T \leqslant 453$ K. It is interesting to remark that N_u is large: 600 ± 70 B_2O_3 units or 3000 ± 200 atoms. Equation (3) is clearly a way to rationalize the flux dependence of the beam-induced decorrelation time measured in XPCS experiments: N_u is the sample-dependent value that describes the proportionality of τ_X on the inverse average flux and is the real outcome of XPCS measurements in beam-induced conditions. Note that the XPCS relaxation time depends on the scattering volume, being proportional to it. This simply reflects the fact that it takes longer to fluidize a larger amount of atoms.

It is interesting to explore the possibility that the N_u units belong to the same volume V_c. Assuming this volume being spherical, its radius ξ will be related to N_u by the relation

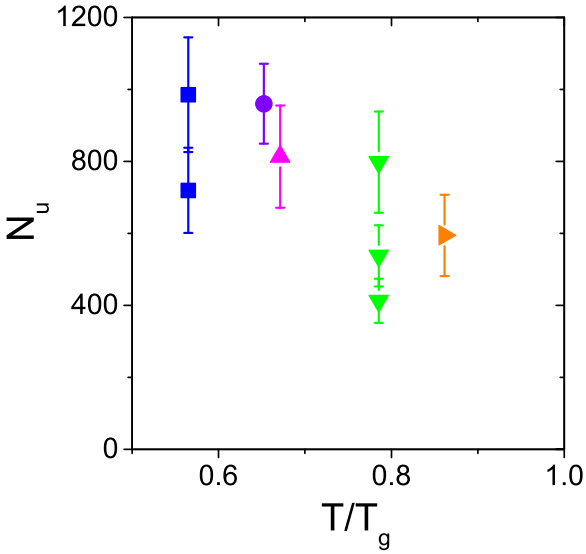

FIG. 7. Temperature dependence of the number of B_2O_3 units that move following an x-ray absorption event. Same symbols as in Fig. 6.

$\xi = \sqrt[3]{3N_u v_{B_2O_3}/4\pi}$, where $v_{B_2O_3}$ corresponds to the volume of a B_2O_3 unit. We obtain a value of $\xi = 2.3 \pm 0.1$ nm at $T = 297$ K. It is suggestive to observe that this value is similar to those reported for the cooperativity length ξ_α at the glass transition temperature ($\xi_\alpha = 2.0$ nm [25] and 1.5 nm [26]). We can hypothesize the following mechanism as responsible for the beam-induced dynamics. The absorption of one photon generates a photoelectron which gives rise to a radiolysis-induced atomic displacement with a given probability [27–30]; however, since a glass is a metastable system characterized by internal stresses, this atomic displacement cannot be accommodated on its own and will be rather accompanied by the rearrangement of a larger region, corresponding to the cooperative volume. A similar mechanism of stress release generated by random bond breaking has been recently exploited in numerical simulations of soft solids [31] to probe their slow dynamics and was found responsible for the emergence of compressed correlation functions and of superdiffusivity.

It is also tempting to recognize, despite the large scattering of the present data, a temperature dependence for N_u, and thus for ξ, in Fig. 7, ξ is possibly decreasing on increasing T as is expected for the cooperative length measured in the liquid phase [32,33]. Although this idea needs to be confirmed by experiments on more materials and validated in detail, it is clear that alternative schemes can also be imagined to explain the value that we obtain for N_u. Considering, in fact, that the primary electrons produced by photoelectric absorption have an energy of about 8 keV and assuming a few tens of eV as the average energy loss per inelastic collision of the primary electron [34], we can estimate that up to a few hundred inelastic collisions per absorption event have the potential to give rise to atomic displacement by radiolysis. Although this number is an order of magnitude smaller than the number of atomic displacements corresponding to N_u, it is possible (although unlikely) that all of these inelastic collisions give rise to the angstrom-long displacements detected here, and, therefore, that each radiolysis event leads to the displacement of about ten atoms. Also, in this scenario, there is some cooperativity required for the atomic displacements due to radiolysis, although clearly on a different length scale as the one discussed above.

IV. CONCLUSIONS

To summarize, we have investigated, in some detail, the effect of a hard x-ray beam on a borate glass using XPCS. In the supercooled liquid, we probe the spontaneous dynamics related to the structural relaxation at the atomic length scale; in the glassy state, instead, the x-ray beam gives rise to a beam-induced dynamics. The x-ray beam thus fluidizes the sample: It induces local changes, and the overall configuration is renewed after the decay time τ_X. These results confirm and extend to a new class of oxide glasses, those already reported in Ref. [14]; different from that case, however, the shape of the correlation functions remains basically exponential instead than compressed.

Moreover, the beam-induced and the structural relaxation characteristic times are here shown to compete with each other, and the two processes take place in parallel so that the shorter one dominates the observed dynamics. We also confirm the proportionality between the induced-dynamics characteristic time and the inverse of the average flux of the x-ray beam impinging on the sample reported in Ref. [14]. We show here that this proportionality can be interpreted in terms of a fixed amount of material that rearranges after a one-photon absorption event. The obtained value for this amount of material turns out to be similar to that expected for dynamical heterogeneities and actually rather close to the available estimates for B_2O_3 [25,26]. This observation, when confirmed for other glasses, would establish a useful connection between the x-ray beam-induced dynamics here observed and a property of large interest for glasses.

ACKNOWLEDGMENTS

The XPCS data here reported have been collected during one experiment at the ESRF (Proposal No. HC1735). We thank C. Armellini for help during the preparation of the sample. We acknowledge the ESRF for the provision of synchrotron radiation facilities and thank Y. Chushkin and K. L'Hoste for assistance in using beamline ID10.

[1] G. Grübel, A. Madsen, and A. Robert, *Soft-Matter Characterization* (Springer, Berlin, 2008), p. 953.

[2] M. Sutton, S. G. J. Mochrie, T. Greytak, S. E. Nagler, L. E. Berman, G. A. Held, and G. B. Stephenson, Nature (London) **352**, 608 (1991).

[3] S. Brauer, G. B. Stephenson, M. Sutton, R. Brüning, E. Dufresne, S. G. J. Mochrie, G. Grübel, J. Als-Nielsen, and D. L. Abernathy, Phys. Rev. Lett. **74**, 2010 (1995).

[4] A. Madsen, A. Fluerasu, and B. Ruta, *Synchrotron Light Sources and Free-Electron Lasers* (Springer, Berlin, 2015), p. 1617.

[5] G. B. Stephenson, A. Robert, and G. Grübel, Nature Mater. **8**, 702 (2009).
[6] M. Leitner, B. Sepiol, L.-M. Stadler, B. Pfau, and G. Vogl, Nature Mater. **8**, 717 (2009).
[7] W. H. Zachariasen, J. Am. Chem. Soc. **54**, 3841 (1932).
[8] B. E. Warren, Phys. Rev. **45**, 657 (1934).
[9] K. J. Rao, *Structural Chemistry of Glasses* (Elsevier, Amsterdam, 2002).
[10] M. D. Ediger, C. A. Angell, and S. R. Nagel, J. Phys. Chem. **100**, 13200 (1996).
[11] B. Ruta, Y. Chushkin, G. Monaco, L. Cipelletti, E. Pineda, P. Bruna, V. M. Giordano, and M. Gonzalez-Silveira, Phys. Rev. Lett. **109**, 165701 (2012).
[12] B. Ruta, G. Baldi, Y. Chushkin, B. Rufflé, L. Cristofolini, A. Fontana, M. Zanatta, and F. Nazzani, Nat. Commun. **5**, 3939 (2014).
[13] V. M. Giordano and B. Ruta, Nat. Commun. **7**, 10344 (2016).
[14] B. Ruta, F. Zontone, Y. Chushkin, G. Baldi, G. Pintori, G. Monaco, B. Rufflé, and W. Kob, Sci. Rep. **7**, 3962 (2017).
[15] M. A. Ramos, J. A. Moreno, S. Vieira, C. Prieto, and J. F. Fernández, J. Non-Cryst. Solids **221**, 170 (1997).
[16] J. A. Bucaro and H. D. Dardy, J. Appl. Phys. **45**, 2121 (1974).
[17] D. Lumma, L. B. Lurio, S. G. J. Mochrie, and M. Sutton, Rev. Sci. Instrum. **71**, 3274 (2000).
[18] Y. Chushkin, C. Caronna, and A. Madsen, J. Appl. Crystallogr. **45**, 807 (2012).
[19] G. Williams and D. C. Watts, Trans. Faraday Soc. **66**, 80 (1970).
[20] W. Götze and L. Sjögren, Rep. Prog. Phys. **55**, 241 (1992).
[21] B. Ruta, G. Baldi, F. Scarponi, D. Fioretto, V. M. Giordano, and G. Monaco, J. Chem. Phys. **137**, 214502 (2012).
[22] F. Dallari, B. H. Kintov, G. Pintori, F. Riboli, F. Rossi, C. Armellini, M. Montagna, and G. Monaco, Philos. Mag. **96**, 800 (2016).
[23] Z. Evenson, B. Ruta, S. Hechler, M. Stolpe, E. Pineda, I. Gallino, and R. Busch, Phys. Rev. Lett. **115**, 175701 (2015).
[24] M. Ross, M. Stana, M. Leitner, and B. Sepiol, New J. Phys. **16**, 093042 (2014).
[25] L. Hong, V. N. Novikov, and A. P. Sokolov, J. Non-Cryst. Solids **357**, 351 (2011).
[26] E. Hempel, G. Hempel, A. Hensel, C. Schick, and E. Donth, J. Phys. Chem. B **104**, 2460 (2000).
[27] D. L. Griscom, Proc. SPIE **0541**, 38 (1985).
[28] G. H. Kinchin and R. S. Pease, Rep. Prog. Phys. **18**, 1 (1955).
[29] L. W. Hobbs, F. W. Clinard, S. J. Zinkle, and R. C. Ewing, J. Nucl. Mater. **216**, 291 (1994).
[30] L. Calliari, M. Dapor, L. Gonzo, and F. Marchetti, in *Desorption Induced by Electronic Transitions DIET IV*, edited by G. Betz and P. Varga, Springer Series in Surface Sciences Vol. 19 (Berlin, Springer, 1990), p. 373.
[31] M. Bouzid, J. Colombo, L. V. Barbosa, and E. Del Gado, Nat. Commun. **8**, 15846 (2017).
[32] G. Adam and J. H. Gibbs, J. Chem. Phys. **43**, 139 (1965).
[33] E. Donth, J. Non-Cryst. Solids **53**, 325 (1982).
[34] R. F. Egerton, Microsc. Res. Tech. **75**, 1550 (2012).